Surface Engineering: Optimization of Antigen Presentation in Self-Assembled Monolayers

Claus Duschl,* Anne-Françoise Sévin-Landais,*‡ and Horst Vogel*
*Institut de Chimie Physique IV, Ecole Polytechnique Fédérale de Lausanne, CH-1015 Lausanne, Switzerland, and ‡Institut de Biochimie, Université de Lausanne, CH-1066 Epalinges, Switzerland

ABSTRACT The formation of self-assembled monolayers (SAMs) on gold surfaces containing an antigenic peptide $(NANP)_6$ and $HS(CH_2)_{11}OH$, and the specific binding of a monoclonal antibody to these layers were investigated by surface plasmon resonance (SPR). Peptides were synthesized by solid-state phase synthesis and were linked either to cysteine or to an alkyl-thiol to allow covalent attachment to gold. The content of the peptide in the SAMs was systematically varied, and the binding properties of the monoclonal antibody were compared with those measured by microcalorimetry in solution. At a critical peptide concentration in the SAM an optimal antibody binding and complete surface coverage was attained. At lower peptide concentrations, the amount of adsorbed antibody decreased; at higher peptide concentrations, the binding constant decreased. These effects can be explained if the accessibility of the antigenic epitopes depends on the peptide density. Addition of free antigen induced the desorption of bound antibodies and allowed accurate measurements of the dissociation rate constant. Binding constants obtained from steady-state measurements and from measurements of the kinetic rate constants were compared.

INTRODUCTION

The understanding of recognition and binding between biological receptor proteins and various ligands (antigen-antibody, receptor-ligand) on a molecular level is a central issue in modern biology. In living organisms many such binding events occur close to or directly at interfaces, namely on cell membranes (Cold Spring Harbor Laboratory, 1992): many receptor molecules are transmembrane proteins that bind their ligands in the immediate vicinity of the membrane surface, and the immuno-response of antibodies against bacteria or viruses is very often directed toward surface proteins, to mention only two examples. Interfaces impose additional restrictions on the interactions of binding partners when compared to binding in solution (Andrade and Hlady, 1986). It is of paramount importance to understand these implications for two reasons: to obtain a more profound understanding of the basic mechanisms involved in signal transduction across cell membranes and for the construction of artificial cell membranes on solid supports for the development of biospecific sensor surfaces. In this context, many important aspects have been addressed in the literature:

- The diffusion of ligands and receptors at and within the membrane modifies the probabilities of association and dissociation phenomena (Adam and Delbrück, 1968; Berg and Purcell, 1977; Ortega et al., 1991).
- Multivalent binding causes modifications of the binding constants (Parce et al., 1979; Pisarchick and Thompson, 1990; Petrossian and Owicki, 1984). In this context the binding of large ligands covering several potential binding sites has also been considered (Stankowski, 1983; Tamm and Bartoldus, 1988). Both aspects are highly dependent on the distribution and mobility of the binding sites on the surface.
- Nonspecific interactions between the ligand and the surface might not only alter the specificity of the reaction but might also modify the binding constants measured.

The aim of this paper is to study the influence of the accessibility of an antigenic peptide immobilized on a gold surface and to optimize its presentation with respect to the binding properties of a monoclonal antibody against this peptide (see Fig. 1). Additionally, the determination of the nonspecific response due to the binding of a nonspecific antibody should allow the specificity of such functionalized organic surfaces to be perfected. The problems encountered when kinetic dissociation rate constants are measured on surfaces are also discussed.

To optimize specific molecular recognition on a surface, several problems must be addressed:

- The binding site of the peptidic receptor must be optimally presented, i.e., the antibody to be bound must have free access to the binding site, as in solution. In general, this is not the case when a peptide is bound to the surface, because steric problems can arise due to a dense packing of the molecules on the surface. Second, if the peptide does not protrude far enough into the solution, the binding pocket of the antibody may not be able to approach the antigen sufficiently (Spinke et al., 1993).
- Because many transducing techniques are not intrinsically specific, the modified surface should allow only specific binding. Therefore all attractive interactions (electro-

Received for publication 29 September 1995 and in final form 19 January 1996.

Address reprint requests to Dr. Claus Duschl, Institut de Chimie Physique IV, Ecole Polytechnique Fédérale de Lausanne, CH-1015 Lausanne, Switzerland. Tel.: 41-21-693-6168; Fax: 41-21-693-6190; E-mail: duschl@icphp1.epfl.ch.

0006-3495/96/04/1985/11 $2.00

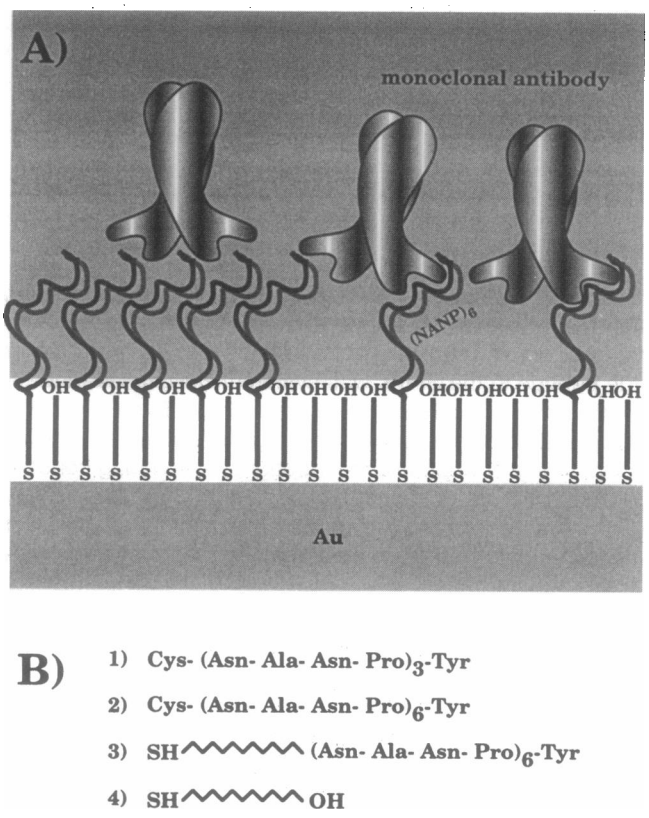

FIGURE 1 (*A*) Schematic representation of the self-assembled monolayer containing 11-mercaptoundecanol and $HS(CH_2)_{11}$-$(NANP)_6Y$. The lower peptide content (*right*) should show improved accessibility of the binding sites of the antibodies. (*B*) Structural formula of the compounds used in this work.

static, van der Waals, hydrophobic) that lead to nonspecific binding between proteins and the active surface must be minimized, and the remaining attractions must be counterbalanced by repulsive forces (Jeon et al., 1991).

A contribution to the suppression of nonspecific binding might come from these peptides themselves. When water-soluble polymers (e.g., ethylene oxides) are immobilized by having one end attached to a solid support, they can align preferentially normal to the surface (grafted polymers). When a protein approaches such a surface, the configurational degrees of freedom of the polymers are reduced. This entropic effect leads to a net repulsion of the protein if the van der Waals attraction, described by the Hamacker constant (Israelachvili, 1991), is weak. Ethylene oxides fulfill these conditions and are therefore very effective in preventing nonspecific binding (Jeon et al., 1991). Because the peptides used here are also water-soluble polymers, they might behave in the same way as the polyethylene oxides, provided that their Hamacker constant is small. By designing the active sensing surface with extended water-soluble peptides as described, it might thus be possible not only to achieve optimal presentation of the binding site but also to ensure effective suppression of nonspecific adsorption.

The experimental approach of this work is based on i) the synthesis of sulfur-containing, antigenic peptides, ii) the formation of SAMs (Bain and Whitesides, 1989b) on gold containing these peptides, and iii) the use of surface plasmon resonance (SPR) (Knoll, 1991; Fägerstam et al., 1992) as a surface-sensitive analytical technique.

i) The model peptides synthesized (see Fig. 1) consist of three or six units of the sequence NANP (Asn-Ala-Asn-Pro). These segments were linked at the N-terminus, either to a cysteine residue or to a hydrocarbon chain (C_{11}) with a terminal thiol group, allowing in both cases covalent binding to the gold surface. The NANP sequence was chosen as an antigenic sequence because of its relevance for the immune response against malaria parasites. The circumsporozoite protein uniformly surrounds the human malaria parasite (Godson, 1985) and consists of a major tandem repetitive amino acid sequence, NANP, flanked by nonrepetitive sequences (Nussenzweig and Nussenzweig, 1989). The NANP repeats seem to present the main target of the antibody response induced by sporozoites after natural or experimental infections. Therefore, by covering the gold substrate with NANP peptides, we intended to mimic the surface of the human malaria parasite.

ii) It has been shown that alkyl thiols of sufficient length form well-defined ordered monolayers on gold substrates (Bain et al., 1989). The use of an alkyl spacer containing 11 carbons should allow control of the orientation of the antigenic peptide sequence on the surface. The surface coverage of the peptide can then be controlled by co-adsorption of alkyl thiols of the same length as the linker. The goal is a molecular arrangement in which the peptides protrude from a densely packed, well-organized monolayer to be approached by the antibodies. The alkyl thiols bear hydroxyl groups, which are exposed to the solution in the completed monolayer. These groups are very effective in screening the hydrophobic contributions of the gold substrate and the alkyl chains and therefore suppress nonspecific binding (Prime and Whitesides, 1991). Because these layers are uncharged, we expect only weak electrostatic interactions to occur.

iii) SPR allows in situ monitoring of the kinetics of layer formation and the binding of antibodies at a gold/buffer interface. The evanescent electromagnetic field of the surface plasmon probes the optical properties in the vicinity of the metal surface. The resonance condition for the excitation of the surface plasmons is highly sensitive to the mass coverage on the surface and enables a quantitative determination of the amount of adsorbed molecules per unit area.

Here we report on the formation and characterization of pure and mixed peptide layers in which the composition was systematically altered. The association kinetics and the amount of specific and nonspecific antibody binding on these layers have been measured. An improved experimental approach is demonstrated for the measurement of the dissociation rate constants of bound antibody on planar surfaces: the addition of free water-soluble $C(NANP)_6Y$ triggers the desorption of bound antibodies and allows reliable determination of this kinetic parameter. Finally, the

measured rate and binding constants are discussed in the context of the above-mentioned aims of this work.

MATERIALS AND METHODS

Chemical synthesis

Fig. 1 shows the structural formulas of the thiol adsorbates 1, 2, 3, and 4, which were synthesized as described below.

Peptides were synthesized by solid-phase strategy (Atherton et al., 1979) on an automated multiple synthesizer (Applied Biosystems) on a 0.1–0.2-mmol scale. Wang resin was used and was functionalized with TyrOH (0.44 mmol/g). Coupling of the appropriate Fmoc amino acids was performed using HOBT/DICI in DMF. Asn and Cys were introduced as triphenylmethyl protected amino acids. When Asn was the last amino acid to be coupled, AsnOH was used. The alkyl spacer in 3 $(HS(CH_2)_{11}$-$(NANP)_6Y)$ was introduced as 11-triphenylmethylthioundecanoic acid (see below for synthesis) using HOBT/DICI for coupling. For Fmoc deprotection, piperidine in DMF was used. After synthesis, the peptides were cleaved from the resin and side-chain deprotected with TFA/water/Et_3SiH (92.5/2.5/5, 2 h). After ether precipitation and lyophilization, peptides were purified by high-performance liquid chromatography on a reverse-phase column (permacoat RP6). They were further subjected to amino acid and mass spectrum analysis.

11-Mercaptoundecanoic acid and 11-mercaptoundecanol were synthesized according to the methods of Troughton et al. (1988) and Bain et al. (1989), respectively. 11-Triphenylmethylthioundecanoic acid was prepared by warming 11-mercaptoundecanoic acid with triphenylmethylbromide (1.2 eq) to 50°C in DMF for 30 min. The mixture was then diluted with ether and washed with sodium acetate 10% in water. Purification by flash chromatography (ether/petroleum ether, 1/9 to 5/5) afforded the desired compound (70%).

Formation of SAMs and binding of antibodies

Self-assembly of peptides and of peptide-thioalcohol mixtures (concentration ratios from 0.5 to 60 mol% peptide) were performed in the teflon cell in water and in 1:1 ethanol-water mixture, respectively, at a total concentration of 3.8 10^{-3} M. The binding was monitored in situ using surface plasmon resonance. Once an apparent steady state was reached (usually after 2 h), the surface was extensively washed with water or ethanol-water mixture, and the final angle shift corresponding to the mass loading was measured. Immuno-reaction experiments were then performed by incubation of the peptide-thioalcohol monolayer with a defined concentration of monoclonal antibody E9 (specific binding) or of polyclonal rabbit IgG (1.2 10^{-6} M, nonspecific binding) in phosphate buffer (pH = 7) until a steady state was reached (usually 1 h). The surface was washed with phosphate buffer and the final thickness measured. A slightly different procedure was used to obtain the thickness values with low concentrations of antibodies ($\leq 10^{-8}$) for the determination of the binding isotherm: to compensate for the depletion of antibodies in solution through binding, it was necessary to incubate the surface several times with a solution of the same concentration until a steady state was reached (about 3 h). Therefore, in all cases, the applied concentrations correspond to the concentrations of free antibodies (c_{Ab}) according to the mass action law.

The desorption of the antibody was initiated through addition of water-soluble $C(NANP)_6Y$ in excess (10^{-4} M in phosphate buffer), and the time course was recorded. After 2 h, the layer was rinsed with phosphate buffer and the final angle shift recorded.

For the self-assembly and the binding experiments deionized water (Nanopure, 18 MΩm) was used, and all the solvents were of UV quality.

Surface plasmon resonance

In an attenuated total reflection (ATR) scan, the excitation of the surface plasmon waves is observed as a pronounced dip in the reflectivity. The optical properties of the thin organic film were derived by fitting the experimental reflectivity-versus-angle (θ-2θ) scans with curves calculated according to the Fresnel equations. For all given thicknesses a refractive index $n = 1.45$ was used. The time-dependent measurements were taken at a fixed angle slightly smaller than the resonance angle, at the steepest part of the resonance curve. A shift of the reflection minimum to greater angles due to the adsorption of an organic layer caused an increase in the measured reflectivity.

The surface plasmon resonance measurements were performed, using the Kretschmann coupling scheme (Kretschmann, 1972), on a home-made computerized reflection apparatus as described in detail elsewhere (Terrettaz et al., 1993). At the resonance angle, the incident laser beam (He-Ne laser, 632.8 nm, p-polarized) couples via an equilateral, high-index prism (SF 10, $n = 1.723$) to the surface plasmon mode in a thin gold film.

Microcalorimetry

Calorimetric experiments were performed with an OMEGA titration calorimeter (MicroCal, Northampton, MA). This instrument has been described in detail by Wiseman et al. (1989). All solutions were thoroughly degassed by stirring under vacuum before use. Peptide and antibody samples were prepared in phosphate-buffered saline (PBS) buffer (pH 7) of the same batch to minimize artifacts due to minor differences in buffer composition. Antibody Sp3E9 (287 μl of a 9.8 mg/ml solution in PBS) was placed in the reaction cell in PBS buffer (2.2 ml). A 0.3 mM solution of $HS(CH_2)_{11}$-$(NANP)_6Y$ in the same buffer was then injected from a 100-μl syringe at 5-min intervals in 16 portions of 5 μl each, with stirring at 400 rpm. Assuming the two binding sites of an antibody to be independent, the binding constant (K), the binding enthalpy (ΔH), and the stoichiometry (n) could be independently determined. Data analysis was carried out with the software provided with the instrument (Wiseman et al., 1989).

RESULTS

SAMs containing NANP

We first measured the thickness of different self-assembled layers on gold in which the antigenic NANP sequence was present.

The first set of experiments was performed using $C(NANP)_6Y$ or $C(NANP)_3Y$ directly attached to the gold surface via the thiol group of the cysteine residue. The thickness of the layer formed was found to be 33 Å for the $C(NANP)_3Y$ layer and 35 Å for the $C(NANP)_6Y$ layer. From these measurements an area per molecule can be derived using a refractive index increment ($dn/dc = 0.18$) (CRC Press, 1973). Assuming a cylindrical shape for the molecule, the diameter (d) and the height (h) of the cylinders were determined in both cases. The fact that the ratios h/d are very similar for the two peptides (~3.5) clearly indicates similar conformations of the peptides in the monolayers.

We then studied mixed self-assembled monolayers containing $HS(CH_2)_{11}OH$ and $HS(CH_2)_{11}$-$(NANP)_6Y$. These SAMs were prepared by incubating a series of gold slides with solutions of different mixing ratios of both substances as described above. In general, the composition of the film is not necessarily identical to that of the solution (Bain and Whitesides, 1989a). However, measurement of the film thickness by surface plasmon resonance allowed quantification of the variation of the mixing ratio. For convenience,

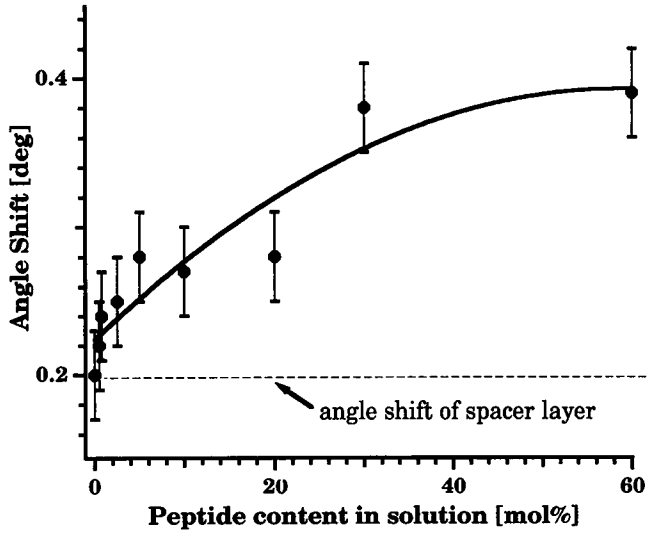

FIGURE 2 Angle shift on co-adsorption of $HS(CH_2)_{11}$-$(NANP)_6Y$ and HS-$(CH_2)_{11}$-OH versus their molar composition in solution. The angle shift of 0.2° corresponds to a layer thickness of 13 Å using a refractive index n = 1.45. The solid line is a least-squares fit using a third-order polynomial.

we will use, if not otherwise stated, throughout this paper the notation X mol% peptide layer to refer to the composition of the solution used for incubation.

As shown in Fig. 2, the angle shifts due to the layer formation varied from 0.2° for a pure 11-mercaptoundecanol layer to 0.39° for a 60 mol% peptide layer. It is worth noticing that the film thicknesses vary with time: after self-assembly of a 2.5 mol% peptide layer for 24 h, it was observed that the angle shift increased from 0.24° (2 h) to 0.29° (24 h), indicating an enrichment in peptide with time. Because of this time dependence of the composition of the film, all presented experiments (apart from the measurement of the binding isotherm) had a fixed time of monolayer self-assembly of 2 h.

From the thickness measurements of pure $C(NANP)_6Y$ layers and pure thioalcohol layers, one can derive the actual composition of the different mixed films. For this purpose, we assume that the layer is divided into two parts: an alkyl chain whose thickness remains constant (0.2°) and a peptidic part whose thickness varies with composition. The area per peptide of the mixed layer is then calculated from the thickness ratio of the pure $C(NANP)_6Y$ layer and the peptidic part of the mixed layer. Assuming an area of 20 $Å^2$ for every alkyl chain, we are able to derive a real film composition (Table 1). As Table 1 shows, for low peptide content, the composition of the film is very close to that of the solution used for self-assembly. With increasing peptide content, deviation between the two compositions increases. There are three possible reasons for this: different solubilities or different diffusion constants of the two adsorbates, or steric hindrance of the peptides adsorbing on the surface.

TABLE 1 Comparison of thin film and solution molar compositions

$HS(CH_2)_{11}$-$(NANP)_6Y$ content in solution (mol%)	$HS(CH_2)_{11}$-$(NANP)_6Y$ content in the SAM (mol%)
0.5	0.5
2.5	1.3
10	2.7
20	4.2
30	5.3
60	6.7

Antibody binding

Incubation of the peptide-thioalcohol monolayer was performed with three different concentrations (1.2×10^{-7}, 4.7×10^{-7}, and 9.4×10^{-7} M) of monoclonal antibody E9 to compare the binding capacities of the different layers. These concentrations were chosen because they are close to the dissociation constant found in solution (cf. calorimetric measurement). Indeed, under these conditions, slight variations in the composition of the self-assembled monolayer are emphasized by considerable variation in the amount of antibody bound to the surface. Fig. 3 shows the amount of bound antibody versus the molar composition of the peptide/thioalcohol solution for these three different concentrations.

The maximum amount of bound antibody was observed at around 10 mol% peptide content, irrespective of the antibody concentration. However, this maximum is most prominent for the lowest antibody concentration. Between 0.5 mol% and 10 mol% peptide content, there is a monotonic increase in bound antibody with peptide content. Above 10 mol% peptide content, the binding capability of

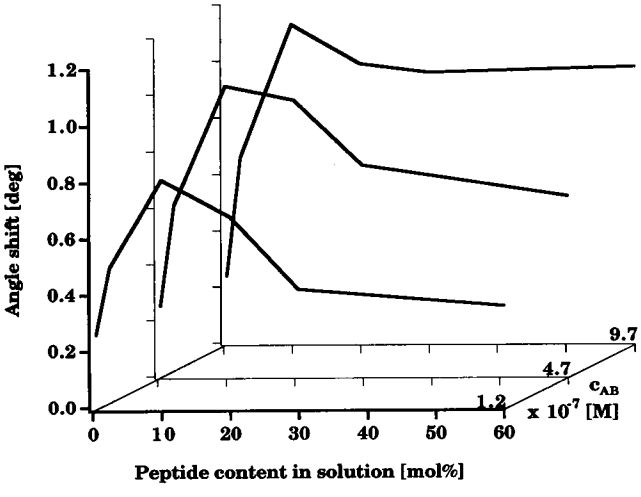

FIGURE 3 Three-dimensional representation of the specific binding of the monoclonal antibody E9 to various peptide-containing SAMs. The angle shift due to the binding of antibodies versus the molar composition of $HS(CH_2)_{11}$-$(NANP)_6Y$ and $HS(CH_2)_{11}OH$ in solution is plotted for different antibody concentrations in solution. An angle shift of 1.0° corresponds to a layer thickness of 64 Å using a refractive index n = 1.45.

the surface decreases drastically until 30 mol%, from which it remains almost constant to 60 mol%.

This graph can also be considered as a three-dimensional representation of binding isotherms of films with different molar composition. To discuss our results in this context, we consider that an angle shift of around 1° corresponds to full coverage of the surface by antibodies. This maximum value can be reached only when the peptide content is around 10%. Below this value, saturation of all antigenic binding sites is observed but does not lead to a complete coverage of the surface by antibodies. For molar composition between 0.5 and 10 mol% $HS(CH_2)_{11}$-$(NANP)_6Y$, an increase of antibody concentration causes only a minor increase in bound antibody. From 10 mol% onward, a saturation of the surface (in a geometrical sense) can be reached only for higher antibody concentrations than applied in the experiments shown.

Within the antibody concentration range used, different parts of the binding isotherms for each film are covered: going from the left-hand side to the right-hand side of the graph, we move from saturation to the steepest part of the isotherm. This suggests that the binding constant decreases with increasing peptide content. Indeed, assuming a simple Langmuir behavior for the binding curve, the binding constant K for low-peptide-content films (0.5–10 mol%) must be considerably higher than $8 \times 10^6\ M^{-1}$. For high-peptide-content film (30–60 mol%), K must be around $2 \times 10^6\ M^{-1}$ (see Table 2).

The exact value of K was determined for a film formed from a 5 mol% peptide solution in the following way. The self-assembled mixed layer was successively incubated with solutions of increasing antibody concentration, starting at 10^{-9}M and ending at 10^{-6}M. The affinity constant was evaluated by fitting the binding curve with a Langmuir adsorption isotherm. As shown in Fig. 4, K is $\sim 9 \times 10^7\ M^{-1}$. (Note that the angle shifts measured are higher than those depicted in Fig. 3 for the same solution composition: this is due to 24-h self-assembly of the monolayer, resulting in a higher peptide concentration.)

Using a refractive index increment dn/dc for the adsorbed antibodies from the literature (CRC Press, 1973; Wiley-Interscience, 1989) it is possible to calculate the ratio of immobilized peptides per bound antibody for different compositions of the peptide-containing SAMs. The results are depicted in Fig. 5. For peptide contents up to 2.7 mol% in the SAM (10 mol% in solution) this ratio is constant (between four and five peptides per antibody). At higher peptide concentrations increasing numbers of peptides are needed to bind one antibody.

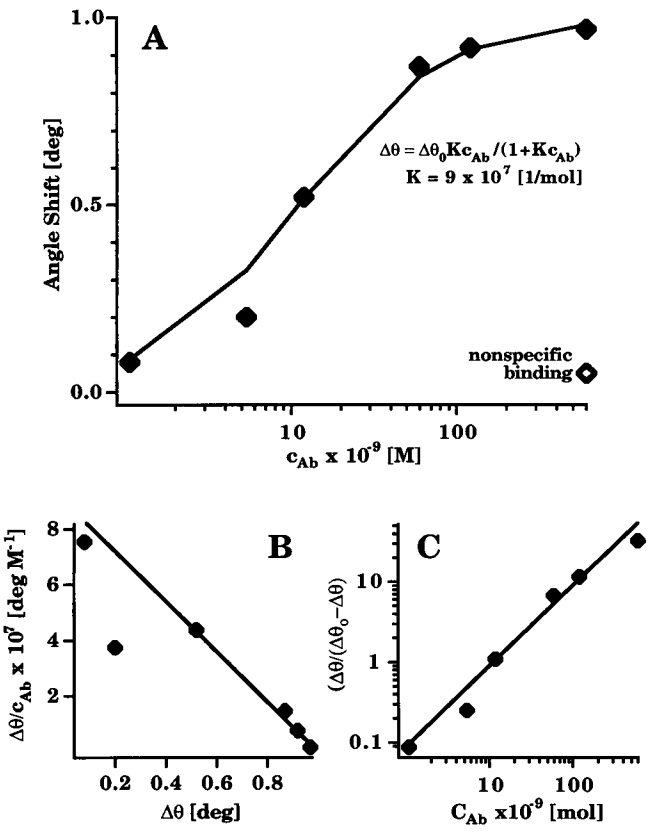

FIGURE 4 Binding curves of the monoclonal antibody E9 on a SAM formed from a solution containing 5 mol% $HS(CH_2)_{11}$-$(NANP)_6Y$. (*A*) Angle shift due to binding of antibodies versus the antibody concentration in solution. The experimental data are represented by the filled diamonds. The full line was calculated using the Langmuir equation and $K = 9 \times 10^7\ M^{-1}$. The open diamond indicates the nonspecific binding using a polyclonal rabbit IgG. (*B*) Scatchard plot and (*C*) Hill plot reveal any deviation from Langmuir binding curve. An angle shift of 1.0° corresponds to a layer thickness of 64 Å using a refractive index $n = 1.45$.

We investigated nonspecific binding using polyclonal rabbit IgG. The nonspecific response was measured both for a pure thioalcohol layer and for a self-assembled layer containing 5 mol% $HS(CH_2)_{11}$-$(NANP)_6Y$ at an IgG concentration of 1.2×10^{-6} M. For the pure thiol layer, an angle shift of 0.23° was obtained, whereas for the peptide-containing layer, the angle shift was 0.05°. When the specific antibody E9 bound to the surface was desorbed by the addition of competing $C(NANP)_6Y$ in solution (see below), there was always a layer of antibodies left, corresponding to

TABLE 2 k_a, k_d, and K for varying compositions of mixed peptide layers

$HS(CH_2)_{11}$-$(NANP)_6Y$ content* (mol%)	k_a ($M^{-1}s^{-1}$)	k_d (s^{-1})	K (M^{-1}) from rate constants	K (M^{-1}) from binding curves‡
0.5	1.2×10^5	7.7×10^{-3}	1.6×10^7	$>1 \times 10^7$
2.5	1×10^5	5×10^{-3}	2×10^7	$>1 \times 10^7$
30	1.2×10^4	6×10^{-3}	2×10^6	$\sim 5 \times 10^6$
60	1.4×10^4	3×10^{-3}	4.7×10^6	$\sim 3.3 \times 10^6$

* Molar content in solution, which is different from that on the surface.

‡ Estimations from the three-dimensional graph in Fig 3.

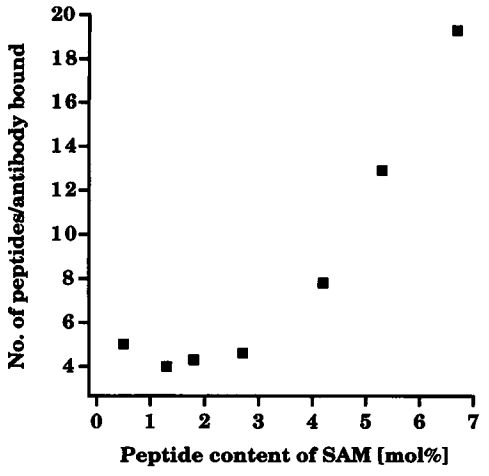

FIGURE 5 Number of peptides of the SAM per bound antibody versus the actual molar composition on the gold surface (not in solution).

an angle shift of 0.1° to 0.2°. The remaining antibodies were obviously much more strongly bound than those that could be displaced by the free $C(NANP)_6Y$.

Microcalorimetric measurements

To compare the binding constants of antibody to antigen measured on the surface with those in solution, we used microcalorimetry. The binding enthalpy, binding ratio, and binding stoichiometry were determined with this technique (see Fig. 6). Because $HS(CH_2)_{11}$-$(NANP)_6Y$ is not soluble in water, the water-soluble $C(NANP)_6Y$ and $C(NANP)_3Y$ peptides were used for the measurements. For these peptides K values of 3.5 ($\pm$0.6) $\times$ 10^7 M^{-1} and 3.9 ($\pm$0.6) $\times$ 10^6 M^{-1}, respectively, were obtained. The values obtained for the stoichiometry (n) and for the binding enthalpy (ΔH) indicate that the monoclonal antibody binds differently to these two peptides: in the case of $C(NANP)_3Y$ the values were n = 2 and ΔH = 20 kcal/mol, whereas for the longer peptide the values gave n = 1.25 and ΔH = 38 kcal/mol. The binding enthalpy measured with $C(NANP)_6Y$ is about two times higher than that measured with the shorter peptide. The fact that the $C(NANP)_6Y$-antibody solution is turbid after the experiment indicates the formation of a network. These results can be explained by assuming that two antibodies can bind to one $C(NANP)_6Y$. It seems unlikely that a single antibody binds to one peptide with two binding sites, because of the small size of the peptides and because of the observed network formation. However, it cannot be ruled out that a minority of the antibodies bind to the peptides in such a way. The measured apparent binding constant should then be a combination of binding constants resulting from the "intrinsic" (one antibody binding site binds to one peptide) binding constant and an increased binding constant due to binding of two binding sites of the same antibody to one peptide (which, when both binding events are independent, would give a binding constant that is the square of the "intrinsic" binding constant).

Kinetic measurements

To find out which of the rate constants (the association rate constant k_a or the dissociation rate constant k_d) causes the variation in K, the binding and desorption kinetics were analyzed. The use of a cuvette without flow-through necessitates the separation of the diffusion processes from the actual rate-constant dependent kinetics of the binding events. For the adsorption process the diffusion can be

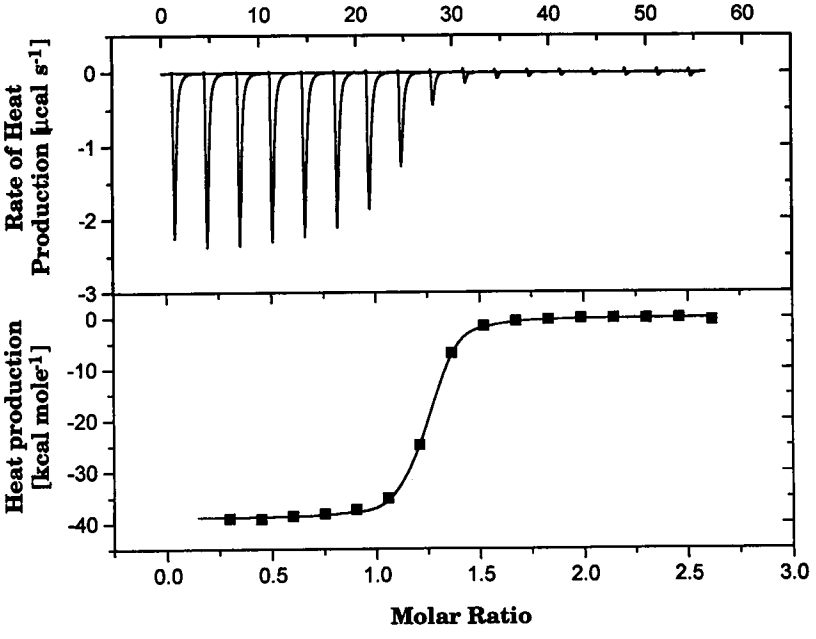

FIGURE 6 Binding curve for $C(NANP)_6Y$ and the monoclonal antibody E9 in solution measured by microcalorimetry. The upper part shows the rate of heat production versus the molar ratio of injected antigen to antibody in the cell volume for every injection. The lower part depicts the integrated heat production versus the same molar ratio. The solid line is a fit as described by Wiseman et al. (1989), who gives the experimental parameters.

described by the following equation (Andrade and Hlady, 1986):

$$n = 2Ac_{Ab}(Dt/\pi)^{1/2}, \quad (1)$$

where n is coverage in number of antibodies adsorbed per unit area; A is a factor that relates the signal in volts to n; c_{Ab} is the concentration of antibodies in solution; D is the diffusion constant of antibodies (10^{-7} cm^2/s); and t is elapsed time.

The experimental adsorption curves were compared with the theoretical curves describing the diffusion for various antibody concentrations in solution (see Fig. 7). There is no free parameter in the theoretical equation. The parts of the curves used for the determination of the rate constants were those that deviated sufficiently from the diffusion-limited behavior. They describe the binding of the antibodies to the antigens in the SAM and follow the rate equation (Karlsson et al., 1991)

$$dI/dt = k_a c_{Ab}(I_{max} - I) - k_d I, \quad (2)$$

where I is the response, which is proportional to the amount of adsorbed antibody; c_{Ab} is the concentration of antibodies in solution; k_a is the association rate constant; and k_d is the dissociation rate constant.

By plotting $(dI/dt)/I$ versus c_{Ab}, we calculated the association rate constants of the binding processes (see Fig. 7, *b* and *c*).

The desorption was initiated by incubating the antibody-covered surface with 10^{-4} M C(NANP)$_6$Y in phosphate buffer (see Fig. 8). The free NANP-peptides compete for the binding sites of the antibodies with the immobilized peptides, and because the concentration of free peptides exceeds that of immobilized peptides by many orders of magnitude, the antibodies are released from the surface. First, we calculated the extent to which diffusion plays a role in this desorption process. If at time $t = 0$, all adsorbed antibodies (N) are simultaneously released from the surface, it can be calculated what fraction (p) of the antibodies is found within 1000 Å of the interface after 1 s. This calculation gives $p = 10^{-3} N$. One second was chosen because it is much shorter than the time constant of the fastest desorption process, and the layer thickness of 1000 Å corresponds to the depth that is probed by the surface plasmon field. Additionally, we calculated whether the diffusion of the free NANP-peptides to the surface is the rate-limiting process. Because it takes 10^{-3} s for N free NANP peptides (N is the number of antibodies bound to the surface for maximum coverage) to adsorb at the interface, one can conclude that this process does not limit the desorption of antibodies either.

The desorption kinetics were fitted with a double exponential, and the fast component was attributed to the k_d (see Fig. 8). The reason why the desorption does not follow a single exponential behavior is not completely clear at the moment and will be discussed below. In Table 2 the k_a, k_d, and K values derived from steady-state binding curves and

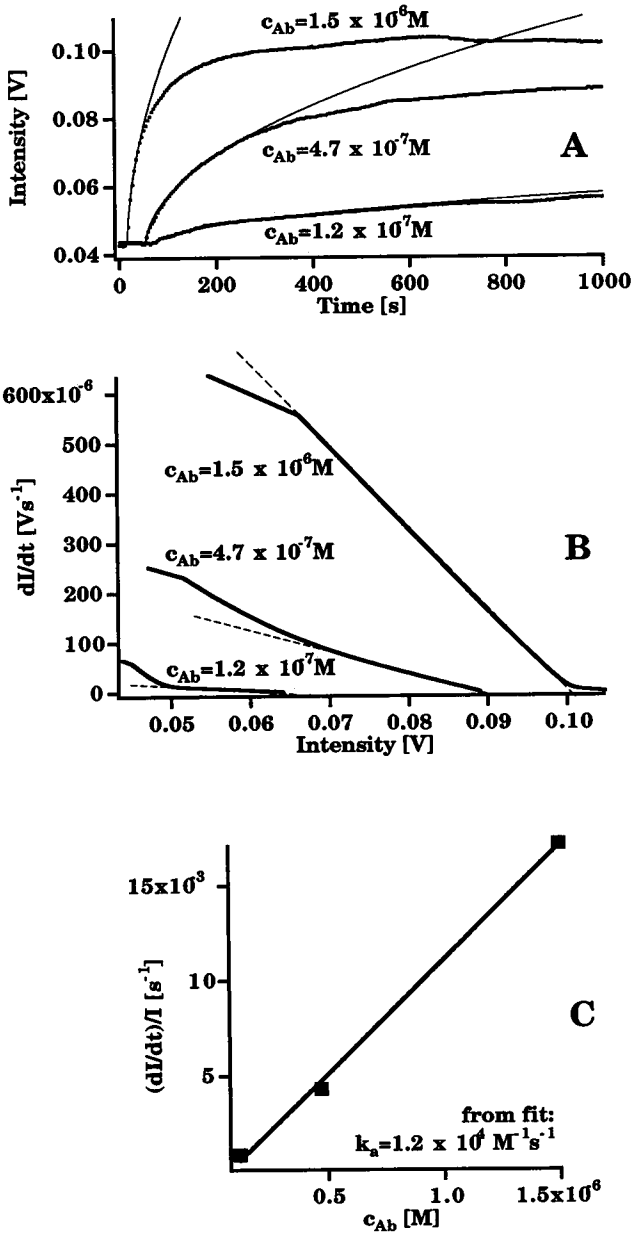

FIGURE 7 Analysis of the kinetic data obtained from the antibody adsorption measurements for various solution concentrations of antibody. The SAM was formed from a solution containing 30 mol% HS(CH$_2$)$_{11}$-(NANP)$_6$Y (the SAM contained 6.7 mol%). (*A*) Increase of the intensity of the reflected light versus time due to the adsorption of antibodies. The dots are experimental data and the thin solid lines are the results obtained on applying the diffusion Eq. 1 to the actual antibody concentrations in solution (see text for details). (*B*) Rate of response (dI/dt) versus the response I for various antibody concentrations. The slopes of the curves used for plot *C* have been taken from the parts that describe the rate-limiting behavior (indicated by the *dotted lines*). (*C*) Slopes $(dI/dt)/I$ versus the antibody concentration in solution. From the slope of the fitted curve (*solid line*), k_a was determined.

from the rate constants are shown for several compositions of the mixed peptide layers. It can be immediately seen that the association rate is different for the different layer systems, and the dissociation rate remains more or less constant for all cases.

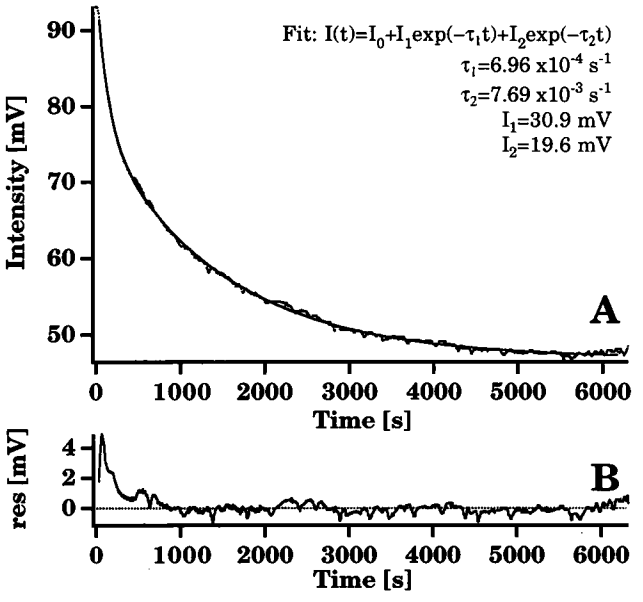

FIGURE 8 Analysis of the kinetic data obtained from the desorption measurement initiated by the addition of a 10^{-4} M C(NANP)$_6$Y solution in buffer. The SAM contained 6.7 mol% HS(CH$_2$)$_{11}$-(NANP)$_6$Y (30 mol% in solution). (*A*) Response I versus elapsed time: the experimental curve (*dots*) was fitted with a double-exponential function (*solid line*). The fit parameters are shown in the graph. (*B*) Residuals of the fit in *A* versus time.

DISCUSSION

Four aspects of our results will be discussed in this section: first, to what extent our results allow a model for the binding mode of the antibodies to be derived; secondly, why we believe that the variable density of peptides on the surface influences the binding constants of the antibody; third, how the desorption process of antibodies from the surface can be triggered through the addition of free antigens in solution. This approach gives better experimental access to the kinetic rate constants, which determine the dissociation of the antibody-antigen complex. Finally, we discuss the role the peptidic chains play in the suppression of nonspecific binding.

Binding mode

The binding constant in solution derived from the calorimetric measurement is smaller by a factor of 2 than that obtained from the surface plasmon experiments (molar composition 5%; see Figs. 4 and 6). Although it is somewhat surprising to find a larger binding constant on the immobilized system (see the Introduction), the difference is within the accuracy of our experiments and we consider the two binding constants to be practically identical.

A more detailed analysis of the binding curve was made with Scatchard and Hill plots (Andrade and Hlady, 1986). These allow the detection of any deviation (cooperativity, presence of different types of binding sites) from a normal Langmuir adsorption isotherm (see Fig. 4). Because neither of these plots indicates any deviation, we conclude that the major fraction of the antibodies bind in a single binding mode to the antigen on the surface.

Additional information about the binding mode can be obtained by calculating the number of peptides (P) per bound antibody for the highest antibody coverage (saturation state of the binding curve for SAMs of low peptide content) (see Fig. 5). This shows that P is between 4 and 5 and increases only for high peptide concentrations (see Table 1). The calculated value of P depends on the assumption that the relationship between mass coverage and refractive index is the same for both the proteins and the peptides (we used the same mass density and the same index increment for both). We are confident that the error is below 30% and is mainly due to the uncertainty in the thickness measurements of the peptide-containing SAMs. If, at high peptide concentrations, both antibody binding sites bind to peptides, one would expect a change in the binding mode upon dilution. On dilution below 10% peptide content (the lowest peptide concentration that still allows complete antibody coverage) there should be a critical peptide density at which the antibodies are not flexible enough to bridge the average distance between two immobilized peptides and P decreases by a factor of 2. At this critical peptide content the binding constant should also abruptly become considerably smaller. In our experiments, however, dilution causes only a decrease in antibody coverage on the surface. From the previous arguments and the fact that P is constant upon dilution of the peptide on the surface, we conclude that the mode of binding remains not only the same for these layer compositions but also that it requires only one antibody binding site per antibody. Only if the binding constant for a 1:2 stoichiometry between the anchored peptides and the antibody is by chance in the same range as the binding constant in solution, and if the binding constant for a 1:1 stoichiometry is at least two orders of magnitude smaller, could we get similar results. In this case, one would expect a two-phase binding curve, reflecting the presence of two different binding constants due to a transition from 1:2 to 1:1 stoichiometry. It is then conceivable that the antibody concentrations applied cover only the flat, intermediate part of the binding curve.

Finally, from our kinetic desorption experiments, a 1:2 stoichiometry should result in a dramatically smaller dissociation constant k_d. The fact that the measured k_d values fit well with data taken from literature in which the diluted immobilization of the peptides in a dextran network drastically reduces the chances that the antibody binds with both binding sites, makes this possibility a rather unlikely one.

These results are somewhat contradictory to the findings of Pisarchick et al. (Pisarchick and Thompson, 1990), who investigated the interaction between monoclonal antibodies and haptens immobilized on a supported lipid bilayer. They found that a considerable fraction of the antibodies bind to two haptens. However, they worked with a system in which a heterogeneous distribution of a much more concentrated hapten content (25%) in the layer might have caused a very

different accessibility of the haptens. In addition, their results might be a consequence of the fact that, unlike our sample where the peptides are fixed to the support via the S-H bond, in their systems the lipid-bound haptens diffuse freely in two dimensions.

Presentation of peptides

We believe, from our results, that the different binding properties of the antibodies on the peptide-covered surfaces (mass coverage, rate constants and binding constants) can be explained by a variable density and accessibility of binding sites on the surface due to differences in the packing of the peptides. We find a critical peptide concentration on the surface (corresponding to a peptide content in solution of 10%) that is sufficient to allow the occupation of all surface sites by the antibody but which is distinguished by the lowest peptide/antibody ratio at full coverage and which gives the optimal binding constant. This should imply that the epitopes of the peptides are presented in such a way that the binding pockets of the antibodies can approach them without having to overcome any steric hindrance. For high peptide concentrations on the surface a decreased binding constant is measured. This, is in our opinion, the consequence of steric hindrance caused by a dense packing of the peptides. Thus the binding pocket of the antibodies (which is topographically slightly hidden inside the protein; Amzel and Poljak, 1979) is sterically repelled by neighboring peptides when it approaches one epitope; this leads to a decrease in the binding constant of the antibody toward the antigen. In this context it is interesting to compare the association rate constants of the antibodies for various peptide concentrations on the surface (see Table 2). The association rate constant k_a is a measure of the probability that an approach of the peptide-antibody system leads to binding. The k_a values decrease by one order of magnitude for high peptide coverages, whereas the dissociation rate constants remain almost constant. Thus the observed decrease in the binding constants for a high peptide coverage is mainly due to a decrease in the association rate constant. It is perhaps surprising that the measured binding curve can be fitted with a simple Langmuir binding isotherm; deviations from the simple model might be expected at high surface coverage. From the presentation of the data in a Scatchard plot it is clear that there are no strong cooperative effects at high coverages.

We did not consider the so-called large ligand effect used by Tamm et al. (Tamm and Bartoldus, 1988). This effect is thought to change the binding properties because of the obstruction of binding sites on adsorption of large proteins. In this context it does not seem justified to attribute a reduced binding constant at high binding site concentrations on surfaces solely to the "large ligand effect," because a reduced accessibility due to dense packing of the peptides should have similar consequences.

For every bound antibody, four to five peptides are necessary. It is not clear why so many peptides are required (van den Heuvel et al., 1993). The most reasonable explanations are either that only a fraction of the peptides is active on the surface or, alternatively, that the peptides are not ideally miscible in the hydroxyl thiols and have a tendency to form patches. As discussed in the previous paragraph, steric obstruction of peptides due to a pure large-ligand effect is unlikely, because a dilution of peptides on the surface should reduce this effect.

Desorption measurements

Measurement of kinetic rate constants is an important and alternative method of probing the binding properties. In general, these measurements are not straightforward to analyze because the diffusion of molecules toward or away from the surface is very often the time-limiting process. The problem of desorption measurements, in particular, is removal of the desorbed antibodies from the surface, so that the actual free antibody concentration in the vicinity of the interface remains practically zero and no rebinding takes place. In this limit the time-dependent desorption curve can then be described with a simple mono-exponential fit. The standard method is to work with a high buffer flow to transport desorbed antibodies away. However, the experimental results very often give a complex time dependence, and only a small fraction of the adsorbed antibodies desorb in a reasonable time (Karlsson et al., 1991; Bernard and Bosshard, 1995). This was also found in our experiments when no free peptide was applied (only 10–15% of the adsorbed antibodies finally desorbed under these conditions; results not shown). We believe that the reason for the incomplete desorption is that, at a certain point in the desorption process, the density of free binding sites on the surface becomes so high that the rebinding of the antibodies is highly favored over diffusion away from the surface (Berg and Purcell, 1977). By incubating an antibody-covered surface with a high concentration of free peptides one can considerably improve this experimental situation because the free antigens compete with the binding sites of the antibodies. Thus a high percentage of desorbed antibodies bind to free peptides in solution, and the probability of rebinding is greatly reduced.

Although we find that this procedure leads to an almost complete desorption of antibodies, the mathematical treatment is complex. A very similar desorption behavior was found in the paper of Panayotou et al. (1993). We believe that the most likely explanation for this is that readsorption still plays a very important role when a considerable number of antibodies have left the surface. Even for high peptide concentrations in solution, there is always a stage where, in the local environment of a newly desorbed antibody, the ratio of unbound immobilized peptides to free peptides becomes high. The probability that an antibody readsorbs increases and the desorption slows down. Similar situations have recently been treated by Ortega et al. (1991) and Goldstein et al. (1989); they performed competition exper-

iments in which, in one case, bound, radioactively labeled antibodies against the type 1 receptor of Fc_ϵ domains were exchanged with a huge excess of nonlabeled antibodies. In the other case, the exchange of haptens between immobilized IgG and soluble IgG was observed. Their theoretical treatment of these processes, taking place at cell membranes, is based on modified rate constants taking into account the influence of diffusion and binding site density, according to the method of Berg et al. (Berg and Purcell, 1977).

The treatment of our data, using a double exponential fit, is solely empirical. It does not reflect the actual functional dependence of the desorption process; however, it gives the simplest description of our data with reasonable fitting residuals. Our initial models of this process suggest that the fast time constant of the fits of the desorption curves can be identified with the molecular dissociation rate constant, whereas the slow time constant reflects the retardation through readsorption of antibodies. The fast time rate that we obtain from these measurements is more than a magnitude of order faster than that measured on the nearly identical system (KKGANP(NANP)$_3$NA − mAb 2A10, $K = 3 \times 10^8$ M^{-1}) (Wohlhueter et al., 1994) on application of a buffer flow. The theoretical treatment of this problem will be the subject of a forthcoming paper.

As previously mentioned, only a small number of antibodies remain on the surface if the antibody-covered surface is incubated with free peptides. It is interesting that the amount of nondesorbing specific antibody correlates well with the amount of nonspecifically adsorbed rabbit IgG (see below). Therefore, it seems likely that the nondesorbing fraction of specific antibodies binds to nonspecific binding sites on the surface (defects), which have very high binding affinities to the antibodies.

Nonspecific binding

Comparison of the binding of a polyclonal rabbit IgG to a pure hydroxythiol layer and to a mixed layer containing 5% $HS(CH_2)_{11}$-$(NANP)_6Y$ shows that the presence of the peptidic chains reduces the amount of nonspecific binding. Because the hydrophilicity should be very similar in both cases, it seems likely that the flexibility of the peptides plays an important role in suppression of the nonspecific adsorption of rabbit IgG. To verify this assumption, one would have to systematically vary the density of the peptides on the surface and measure the nonspecific adsorption of proteins. The determination of the Hamacker constant of the peptides should then allow comparison of the results with recently developed theoretical models (Jeon et al., 1991).

CONCLUSION

Optimization of the presentation of ligands on solid surfaces for the binding of proteins is essential for the design of sensor surfaces. The design and synthesis of appropriate molecules together with the use of established self-assembly techniques allow systematic variation of ligand presentation on a molecular scale. A similar approach was recently used by van den Heuvel et al. (1993). It is possible to optimize the presentation to give sufficient antigen dilution for good accessibility and simultaneously complete antibody coverage of the surface for a high response signal. The desorption of bound antibodies through the addition of soluble antigens improves the determination of the dissociation rate constants. Surface plasmon resonance is ideally suited for monitoring the formation and the binding properties of such functionalized monolayer systems.

The authors thank M. Liley for helpful discussions and for critically reading the manuscript. We are grateful to M. Mutz (Ciba-Geigy, Basel) and L. Leder (Biochemisches Institut der Universität Zürich) for performing the microcalorimetric measurements. We thank H. Matile (Hofmann LaRoche, Basel) and G. Corradin (Institut de Biochimie, Université de Lausanne), who supplied us with the monoclonal antibody E9. We acknowledge the valuable help and advice of G. Corradin for the synthesis of the NANP-peptides.

This work was supported by the Swiss National Science Foundation (SPP Biotechnology).

REFERENCES

Adam, G., and M. Delbrück. 1968. Reduction of Dimensionality in Biological Diffusion Processes. Structural Chemistry and Molecular Biology. A. Rich and N. Davidson, editors. W. H. Freeman, San Francisco. 198–215.

Amzel, L. M., and R. J. Poljak. 1979. Three-dimensional structure of immunoglobulins. *Annu. Rev. Biochem.* 48:961–997.

Andrade, J. D., and V. Hlady. 1986. Protein adsorption and materials biocompatibility: a tutorial review and suggested hypotheses. *Adv. Polym. Sci.* 79:2–63.

Atherton, E., C. J. Logan, and R. C. Sheppard. 1979. Peptide synthesis. Part 2. Procedures for solid phase synthesis using Nα-fluorenylmethoxycarbonyl amino acids on polyamide supports. Sythesis of substance P and of acyl carrier protein 65–74 decapeptide. *J. Chem. Soc. Perkin Trans.* 1:538–546.

Bain, C. D., E. B. Troughton, Y.-T. Tao, J. Evall, G. M. Whitesides, and R. G. Nuzzo. 1989. Formation of monolayer films by the spontaneous assembly of organic thiols from solution onto gold. *J. Am. Chem. Soc.* 111:321–335.

Bain, C. D., and G. M. Whitesides. 1989a. Formation of monolayers by the coadsorption of thiols on gold: variation in the length of the alkyl chain. *J. Am. Chem. Soc.* 111:7164–7175.

Bain, C. D., and G. M. Whitesides. 1989b. Modeling organic surfaces with self-assembled monolayers. *Angew. Chem. Int. Ed. Engl.* 101:522–528.

Berg, H. C., and E. M. Purcell. 1977. Physics of chemoreception. *Biophys. J.* 20:193–219.

Bernard, A., and H. R. Bosshard. 1995. Real-time monitoring of antigen-antibody recognition on a metal oxide surface by an optical grating coupler sensor. *Eur. J. Biochem.* 230:416–423.

Cold Spring Harbor Laboratory. 1992. Cold Spring Harbor Symposia on Quantitative Biology. Cold Spring Harbor, NY.

CRC Press. 1973. Handbook of Biochemistry. H. E. Sober, editor. CRC Press, Cleveland, OH. C-67.

Fägerstam, L. G., Å. Frostell-Karlsson, R. Karlsson, B. Persson, and I. Rönnberg. 1992. Biospecific interaction analysis using surface plasmon resonance detection applied to kinetic, binding site and concentration analysis. *J. Chromatogr.* 597:397–410.

Godson, G. N. 1985. Molecular approaches to malaria vaccines. *Sci. Am.* 5:32–39.

Goldstein, B., R. G. Posner, D. C. Torney, J. Erickson, D. Holowka, and B. Baird. 1989. Competition between solution and cell surface receptors for ligand. *Biophys. J.* 56:955–966.

Israelachvili, J. N. 1991. Intermolecular and Surface Forces, 2nd ed. Academic Press, London, New York.

Jeon, S. I., J. H. Lee, J. D. Andrade, and P. G. d. Gennes. 1991. Protein-surface interaction in the presence of polyethylene oxide. I. Simplified theory. *J. Colloid Interface Sci.* 142:149–158.

Karlsson, R., A. Michaelsson, and L. Mattsson. 1991. Kinetic analysis of monoclonal antibody-antigen interactions with a new biosensor based analytical system. *J. Immuno. Methods.* 145:229–240.

Knoll, W. 1991. Optical characterization of organic thin films and interfaces with evanescent waves. *MRS Bull.* 16:29–39.

Kretschmann, E. 1972. Decay of non-radiative surface plasmon into light on rough silver films. Comparison of experimental and theoretical results. *Opt. Commun.* 6:185–187.

Nussenzweig, V., and R. S. Nussenzweig. 1989. Rational for the development of an engineered sporozoite malaria vaccine. *Adv. Immunol.* 45: 283–334.

Ortega, E., R. Schweitzer-Stenner, and I. Pecht. 1991. Kinetics of ligand binding to the type 1 Fc_ϵ receptor on mast cells. *Biochemistry.* 30: 3473–3483.

Panayotou, G., G. Gish, P. End, O. Truong, I. Gout, R. Dhand, M. J. Fry, I. Hiles, T. Pawson, and M. D. Waterfield. 1993. Interactions between SH2 domains and tyrosine-phosphorylated platelet-derived growth factor β-receptor sequences: analysis of kinetic parameters by a novel biosensor-based approach. *Mol. Cell. Biol.* 13:3567–3576.

Parce, J. W., M. A. Schwarz, J. C. Owicki, and H. M. McConnell. 1979. Kinetics of antibody association with spin-label haptens on membrane surfaces. *J. Phys. Chem.* 83:3414–3417.

Petrossian, A., and J. C. Owicki. 1984. Interaction of antibodies with liposomes bearing fluorescent haptens. *Biochim. Biophys. Acta.* 776: 217–227.

Pisarchick, M. L., and N. L. Thompson. 1990. Binding of a monoclonal antibody and its Fab fragment to supported phospholipid monolayers measured by total internal reflection fluorescence microscopy. *Biophys. J.* 58:1235–1249.

Prime, K. L., and G. M. Whitesides. 1991. Self-assembled organic monolayer: model systems for studying adsorption of proteins at surfaces. *Science.* 252:1164–1167.

Spinke, J., M. Liley, F.-J. Schmitt, H.-J. Guder, L. Angermaier, and W. Knoll. 1993. Molecular recognition at self-assembled monolayers: optimization of surface functionalization. *J. Chem. Phys.* 99:7012–7019.

Stankowski, S. 1983. Large-ligand adsorption to membranes. I. Linear ligands as a limiting case. *Biochim. Biophys. Acta.* 735:341–351.

Tamm, L. K., and I. Bartoldus. 1988. Antibody binding to lipid model membranes. The large-ligand effect. *Biochemistry.* 27:7453–7458.

Terrettaz, S., T. Stora, C. Duschl, and H. Vogel. 1993. Protein binding to supported lipid membranes: investigation of the cholera toxin-ganglioside interaction by simultaneous impedance spectroscopy and surface plasmon resonance. *Langmuir.* 9:1361–1369.

Troughton, E. B., C. D. Bain, G. M. Whitesides, R. G. Nuzzo, D. L. Allara, and M. D. Porter. 1988. Monolayer films prepared by the spontaneous self-assembly of symmetrical and unsymmetrical dialkyl sulfides from solution onto gold substrates: structure, properties, and reactivity of constituent functional groups. *Langmuir.* 4:365–385.

van den Heuvel, D. J., R. P. H. Kooyman, J. W. Drijfhout, and G. W. Welling. 1993. Synthetic peptides as receptors in affinity sensors: a feasibility study. *Anal. Biochem.* 215:223–230.

Wiley-Interscience. 1989. Polymer Handbook, 3rd ed. J. Brandrup and E. H. Immergut, editors. Wiley-Interscience, New York. VII-469.

Wiseman, T., S. Williston, J. F. Brandts, and L.-N. Lin. 1989. Rapid measurement of binding constants and heats of binding using a new titration calorimeter. *Anal. Biochem.* 179:131–137.

Wohlhueter, R. M., K. Parekh, V. Udhayakumar, S. Fang, and A. A. Lal. 1994. Analysis of binding of monoclonal antibody to a malarial peptide by surface plasmon resonance biosensor and integrated rate equations. *J. Immunol.* 153:181–189.